


Cosmological constraints on thermal friction of axion dark matter

Gang Liu^{✉*}, Yuhao Mu, Zhihuan Zhou, and Lixin Xu[†]

*Institute of Theoretical Physics, School of Physics, Dalian University of Technology,
Dalian 116024, People's Republic of China*

 (Received 6 September 2023; revised 19 October 2023; accepted 27 November 2023; published 29 December 2023)

In this paper, we investigate the process in which axion dark matter undergoes thermal friction, resulting in energy injection into dark radiation, with the aim of mitigating the Hubble tension and large-scale structure tension. In the early Universe, this scenario led to a rapid increase in the energy density of dark radiation; in the late Universe, the evolution of axion dark matter is similar to that of cold dark matter, with this scenario resembling decaying dark matter and serving to ease the large-scale structure tension. We employ cosmological observational data, including cosmic microwave background, baryon acoustic oscillation, supernova data, H_0 measurement from SHOES, and S_8 from the Dark Energy Survey Year-3, to study and analyze this model. Our results indicate that the thermal friction model offers partial alleviation of the large-scale structure tension, while its contribution on alleviating Hubble tension can be ignored. The new model yields the value of S_8 is 0.795 ± 0.011 at a 68% confidence level, while the Λ CDM model yields a result of 0.8023 ± 0.0085 . In addition, the new model exhibits a lower χ^2_{tot} value, with a difference of -2.60 compared to the Λ CDM model. Additionally, we incorporate Lyman- α data to reconstrain the new model and find a slight improvement in the results, with the values of H_0 and S_8 being $68.76^{+0.39}_{-0.35}$ km/s/Mpc and 0.791 ± 0.011 at a 68% confidence level, respectively.

DOI: [10.1103/PhysRevD.108.123546](https://doi.org/10.1103/PhysRevD.108.123546)

I. INTRODUCTION

In recent years, an increasing number of observational facts have shown inconsistencies with the predicted results of the Λ CDM model, notably the Hubble and large-scale structure tensions, which may indicate the presence of new physics beyond the standard cosmological model. The Hubble tension refers to the discrepancy between the predicted value of the Hubble constant, H_0 , from the Λ CDM model and the observed value [1,2]. The *Planck* 2018 CMB data yielded a result of 67.37 ± 0.54 km/s/Mpc [3], whereas the SHOES measurement obtained via the distance ladder method at low redshifts resulted in a value of 73.04 ± 1.04 km/s/Mpc [4], with a statistical error of 4.8σ .

The large-scale structure displays a moderate level of tension with CMB, typically quantified by $S_8 \equiv \sigma_8 \sqrt{(\Omega_m/0.3)}$, where σ_8 represents the amplitude of density perturbations, and Ω_m denotes the matter density fraction. The *Planck* 2018 best-fit Λ CDM model yields a value of 0.834 ± 0.016 for S_8 [3]; however, observational results from large-scale structure surveys such as the Dark Energy Survey Year-3 (DES) suggest a lower value of 0.776 ± 0.017 [5].

Various models have been proposed to address these inconsistencies. Common ones include modifying dark energy, including dynamic dark energy [6–8], vacuum phase transition [9–11], early dark energy [12–14], and interacting dark energy [15–20]; modifying dark matter, including partially acoustic dark matter [21], decaying dark matter [22–28], interacting dark matter [29], and axion dark matter [30]. In addition, modification of the gravitational theory is also considered [31–34].

In this paper, we focus on the interaction between dark matter and dark radiation. We investigate this interaction by substituting cold dark matter with axion dark matter, and examine the problem from the perspective of scalar field theory. We consider the impact of additional thermal friction on axion dark matter, which injects energy into dark radiation and alters the evolution equations in the original model of axion dark matter.

Axion dark matter is a potential candidate for dark matter, which can form Bose-Einstein condensates on galactic scales, altering the dynamics of dark matter on small scales while maintaining the success of cold dark matter on large scales [35]. In this paper, we investigate the model of ultra-light axion dark matter, with a mass m_χ approximately at 10^{-22} eV. This particular dark matter model has been extensively studied in previous works [36–38].

Figure 1 presents the influence of axion mass on the matter power spectrum. We keep other cosmological parameters fixed and consistent with the Λ CDM model.

*liugang_dlut@mail.dlut.edu.cn

†lxxu@dlut.edu.cn

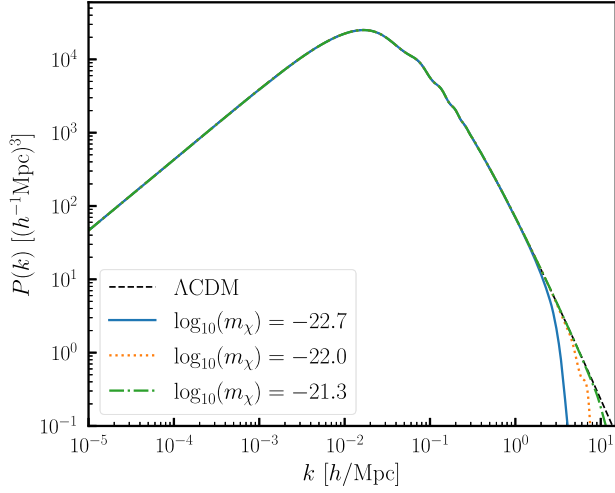


FIG. 1. The impact of axion mass on the matter power spectrum. On large scales, axion dark matter behaves similar to cold dark matter, while on small scales, it exhibits decreased clustering due to condensation. The smaller the axion mass, the more pronounced this effect becomes.

On large scales, the evolution of axion dark matter is similar to that of cold dark matter. However, on small scales, the condensation effect of axion dark matter inhibits structure growth, resulting in a smaller matter power spectrum than that predicted by the Λ CDM model. Furthermore, this effect becomes more apparent as the axion mass decreases.

In the early Universe, the axion field was frozen due to Hubble friction. As the Universe cooled and the Hubble parameter decreased, the axion mass became comparable to the Hubble friction, causing the axion to start rolling and subsequently oscillating near the minimum of its potential. After the axion potential and kinetic energies reach equilibrium, its energy density evolves like that of matter [18,19].

We extend the axion dark matter model by proposing the dissipative axion dark matter (DADM) model, which takes into account the coupling between axion and non-Abelian gauge group. This results in scalar field experiencing thermal friction beyond Hubble friction, transferring energy to the dark radiation composed of dark gauge bosons.

The thermal friction effect of axion has been studied in the context of warm inflation [39–43], late-time dark energy [44,45], and early-time dark energy [46,47]. In this study, we apply it to the realm of axion dark matter.

We constrained the parameters of the DADM model using a combination of various cosmological datasets, including cosmic microwave background (CMB), baryon acoustic oscillation (BAO), supernova data (SNIa), H_0 measurement from SHOES, and S_8 from the Dark Energy Survey Year-3 (DES).

The results indicate that the new model yields the value of H_0 that is close to the result obtained from the Λ CDM

model, while the S_8 in the former is smaller than in the latter. The DADM model yields the value of S_8 is 0.795 ± 0.011 at a 68% confidence level, while the Λ CDM model produces a result of 0.8023 ± 0.0085 . This suggests that the thermal friction model can alleviate the S_8 tension. Additionally, the DADM model demonstrates a lower χ^2_{tot} value, differing by -2.60 compared to the Λ CDM model.

In the analysis of the constraint results, we discovered that the utilization of only the aforementioned five datasets is insufficient to constrain the mass of axion dark matter. Therefore, we fixed the mass of the axion dark matter to be 10^{-22} eV and incorporated Lyman- α data to re-constrain the new model. The results show some improvements, with values of H_0 and S_8 being $68.76^{+0.39}_{-0.35}$ km/s/Mpc and 0.791 ± 0.011 at a 68% confidence level, respectively.

The present paper is structured as follows. In Sec. II, we present the thermal friction model, deduce the evolution equations for both the background and perturbation, and provide the corresponding initial conditions. Section III presents the numerical analysis, including the effects of the model on the background and perturbation levels. In Sec. IV, we describe the data constrained by Markov chain Monte Carlo (MCMC) analyses and provide the results. Finally, in Sec. V, we discuss the findings and offer a conclusion.

II. THERMAL FRICTION MODEL

We extend the Standard Model by introducing a dark non-Abelian gauge group and axion field χ . The dark gauge boson couple to the axion via the operator,

$$\mathcal{L}_{\text{int}} = \frac{\alpha}{16\pi f} \tilde{F}_a^{\mu\nu} F_{\mu\nu}^a, \quad (1)$$

where $F_{\mu\nu}^a$ ($\tilde{F}_a^{\mu\nu} = \epsilon^{\mu\nu\alpha\beta} F_{\alpha\beta}^a$) represents the field strength of the dark gauge boson, α is the fine structure constant, and f denotes the strength of the interaction between axion and the dark gauge field. We consider a simple quadratic potential for the axion,

$$V(\chi) = \frac{1}{2} m_\chi^2 \chi^2, \quad (2)$$

while various forms of axion potential have been studied in previous works [48,49], which can be effectively represented by this quadratic potential [37]. We assume that these two dark sector components interact with other components only through gravity. The conservation of energy-momentum tensor holds for two components,

$$\nabla_\mu T_\chi^{\mu\nu} = -\nabla_\mu T_{\text{dr}}^{\mu\nu}. \quad (3)$$

Using the results from [47,50], we have

$$\nabla_\mu T_{\text{dr}}^{\mu\nu} = g^{\nu\alpha} (-\Upsilon v_{\text{dr}}^\mu \partial_\mu \chi \partial_\alpha \chi), \quad (4)$$

where v_{dr}^μ represents the four-velocity of the dark radiation. The thermal friction coefficient Υ is expected to be correlated with the temperature of dark radiation [51–53]. However, in this paper, we treat Υ as a constant for simplicity and restrict our analysis to the case of weak thermal friction. Investigation of more complex scenarios is left to future work.

A. Background equations

The background evolution equations for the axion dark matter and dark radiation can be derived using Eq. (4),

$$\ddot{\chi} + (3H + \Upsilon)\dot{\chi} + m_\chi^2\chi = 0, \quad (5a)$$

$$\dot{\rho}_{\text{dr}} + 4H\rho_{\text{dr}} = \Upsilon\dot{\chi}^2, \quad (5b)$$

where the dot denotes the derivative with respect to cosmic time, and H is the Hubble parameter. The motion equation of a scalar field includes thermal friction, which results in the transfer of energy from axion to the dark radiation.

The energy density and pressure of the axion dark matter can be expressed as follows:

$$\rho_\chi = \frac{1}{2}\dot{\chi}^2 + \frac{1}{2}m_\chi^2\chi^2, \quad (6a)$$

$$p_\chi = \frac{1}{2}\dot{\chi}^2 - \frac{1}{2}m_\chi^2\chi^2. \quad (6b)$$

We introduce new variables to calculate the equation of motion for the scalar field [37,38,54],

$$\sqrt{\Omega_\chi} \sin \frac{\theta}{2} = \frac{\dot{\chi}}{\sqrt{6}M_{\text{pl}}H}, \quad (7a)$$

$$\sqrt{\Omega_\chi} \cos \frac{\theta}{2} = -\frac{m_\chi\chi}{\sqrt{6}M_{\text{pl}}H}, \quad (7b)$$

$$y_1 = \frac{2m_\chi}{H}, \quad (7c)$$

where $\Omega_\chi = \frac{\rho_\chi}{3M_{\text{pl}}^2 H^2}$ is the density parameter of the dark matter and $M_{\text{pl}} = 2.435 \times 10^{27}$ eV denotes the reduced Planck mass. The evolution equations for the new variable are

$$\frac{\dot{\Omega}_\chi}{\Omega_\chi} = 3H(w_t + \cos \theta) - \Upsilon(1 - \cos \theta), \quad (8a)$$

$$\dot{\theta} = Hy_1 - (3H + \Upsilon) \sin \theta, \quad (8b)$$

$$\dot{y}_1 = \frac{3}{2}Hy_1(1 + w_t), \quad (8c)$$

where w_t represents the total equation of state, which is the ratio of total pressure to total energy density. We can find that the equation of state of axion dark matter is

$$w_\chi = \frac{p_\chi}{\rho_\chi} = -\cos \theta. \quad (9)$$

The continuity equations for axion dark matter and dark radiation can be derived as follows:

$$\dot{\rho}_\chi + 3H\rho_\chi = -\Upsilon\rho_\chi(1 + w_\chi), \quad (10a)$$

$$\dot{\rho}_{\text{dr}} + 4H\rho_{\text{dr}} = \Upsilon\rho_\chi(1 + w_\chi). \quad (10b)$$

After the cessation of axion oscillation (which occurs during the radiation domination epoch), its equation of state $w_\chi = 0$, and the continuity equation takes on the same form as that of decaying dark matter [24–28,55,56]. However, our result is obtained from the scalar field undergoing thermal friction.

Figure 2 depicts the variation of energy density for different components as a function of scale factor. The orange curve represents axion dark matter, which behaves similar to a cosmological constant (blue line) in the early Universe and evolves like matter after undergoing oscillations. Dark radiation (green line) generated by axion thermal friction is negligible in the early Universe. However, due to a continuous source, the dilution rate of dark radiation is slower than that of ordinary radiation (red line) and matter.

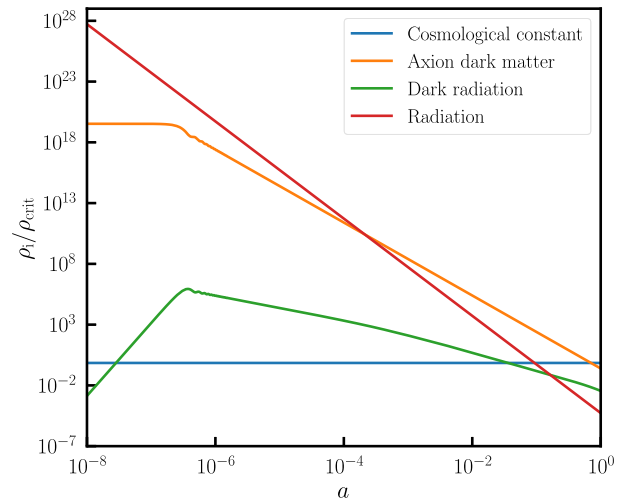


FIG. 2. The energy density of various components of the Universe varies with the scale factor, including ordinary radiation (red line), axion dark matter (orange line), dark radiation (green line), and cosmological constant (blue line). The dark radiation generated by axion thermal friction only has an impact in the late-time Universe.

B. Perturbation equations

We calculated the perturbation equations for axion dark matter and dark radiation with the synchronous gauge, where the line element is defined as

$$ds^2 = -dt^2 + a^2(t)(\delta_{ij} + h_{ij})dx^i dx^j. \quad (11)$$

The perturbed Klein-Gordon equation for a scalar field in Fourier modes is expressed as follows:

$$\delta\ddot{\chi} + (3H + \Upsilon)\delta\dot{\chi} + \left(\frac{k^2}{a^2} + m_\chi^2\right)\delta\chi + \frac{1}{2}\dot{h}\dot{\chi} = 0, \quad (12)$$

where h represents the trace of scalar metric perturbations. In accordance with [57,58], the density perturbation, pressure perturbation, and velocity divergence of axion dark matter can be expressed as

$$\delta\rho_\chi = \dot{\chi}\delta\dot{\chi} + m_\chi^2\chi\delta\chi, \quad (13a)$$

$$\delta p_\chi = \dot{\chi}\delta\dot{\chi} - m_\chi^2\chi\delta\chi, \quad (13b)$$

$$(\rho_\chi + p_\chi)\Theta_\chi = \frac{k^2}{a}\dot{\chi}\delta\chi. \quad (13c)$$

We redefine new variables to calculate the perturbation equation of scalar field [38],

$$\sqrt{\Omega_\chi}\left(\delta_0 \sin \frac{\theta}{2} + \delta_1 \cos \frac{\theta}{2}\right) = \sqrt{\frac{2}{3}}\frac{\delta\dot{\chi}}{M_{pl}H}, \quad (14a)$$

$$\sqrt{\Omega_\chi}\left(\delta_1 \sin \frac{\theta}{2} - \delta_0 \cos \frac{\theta}{2}\right) = \sqrt{\frac{2}{3}}\frac{m_\chi\delta\chi}{M_{pl}H}. \quad (14b)$$

The evolution equations of the new variable can be derived as follows:

$$\begin{aligned} \dot{\delta}_0 &= \delta_0 H\omega \sin \theta - \delta_1 [(3H + \Upsilon) \sin \theta \\ &\quad + H\omega(1 - \cos \theta)] - \frac{\dot{h}}{2}(1 - \cos \theta), \end{aligned} \quad (15a)$$

$$\begin{aligned} \dot{\delta}_1 &= \delta_0 H\omega(1 + \cos \theta) - \delta_1 ((3H + \Upsilon) \cos \theta \\ &\quad + H\omega \sin \theta) - \frac{\dot{h}}{2} \sin \theta, \end{aligned} \quad (15b)$$

where

$$\omega = \frac{k^2}{2a^2 m_\chi H} = \frac{k^2}{a^2 H^2 y_1}. \quad (16)$$

Employing Eq. (4), we derive the perturbed energy density and velocity evolution equations for dark radiation,

$$\begin{aligned} \dot{\delta}_{\text{dr}} &= -\frac{2}{3}\dot{h} - \frac{4}{3a}\Theta_{\text{dr}} \\ &\quad + \Upsilon \frac{\rho_\chi}{\rho_{\text{dr}}} [(\delta_0 - \delta_{\text{dr}})(1 - \cos \theta) + \delta_1 \sin \theta], \end{aligned} \quad (17a)$$

$$\dot{\Theta}_{\text{dr}} = \frac{1}{4a}k^2\delta_{\text{dr}} + \Upsilon \frac{\rho_\chi}{\rho_{\text{dr}}}(1 - \cos \theta) \left(\frac{3}{4}\Theta_\chi - \Theta_{\text{dr}}\right). \quad (17b)$$

It is worth noting that the dark radiation generated by thermal friction experiences sufficient self-interaction to maintain a thermal environment and suppress shear perturbations [47]. In contrast, in most decaying dark matter models, the dark radiation exhibits shear perturbations that cannot be neglected due to the free-streaming [28,56,59,60].

C. Initial conditions

In the very early Universe, the Hubble friction dominates greatly over both the axion mass and thermal friction. When studying the initial conditions of the axion dark matter, the influence of Υ can be neglected, and the scalar field equation simplifies to the case without thermal friction. Therefore, we can directly employ the initial conditions for the new variable of the scalar field presented in [37,38].

We assume that dark radiation is exclusively generated through thermal friction of axion dark matter. Therefore, the initial value of ρ_{dr} is set to zero. For the perturbation equations, we use adiabatic initial conditions,

$$\delta_{\text{dr}} = \frac{3}{4}\delta_\gamma, \quad \Theta_{\text{dr}} = \Theta_\gamma, \quad (18)$$

where the subscript “ γ ” represents the photon.

III. NUMERICAL RESULTS

Based on the description in the last section, we modified the publicly available Boltzmann code CLASS [61,62]. We now present the obtained numerical results and discuss the impact of the DADM model on observations. We employ the parameter values of the Λ CDM model constrained by *Planck* 2018 data,

$$\begin{aligned} \omega_b &= 0.02238, & \omega_{\text{cdm}} &= 0.1201, \\ H_0 &= 67.81, & \ln(10^{10} A_s) &= 3.0448, \\ n_s &= 0.9661, & \tau_{\text{reio}} &= 0.0543. \end{aligned} \quad (19)$$

For the DADM model, we set the axion mass to be 10^{-22} eV and keep all other parameters the same as the Λ CDM model, except for the sum of the dark matter and dark radiation energy density, $\omega_{\text{dm+dr}}$.

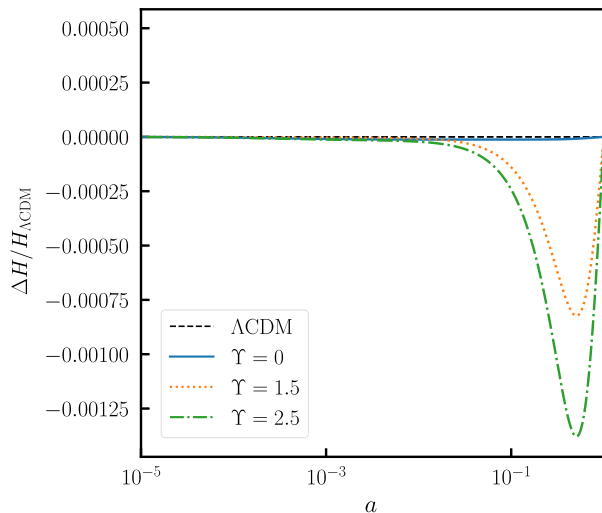


FIG. 3. The evolution of the Hubble parameter relative to the Λ CDM model as a function of the scale factor is depicted for the DADM model under different thermal friction coefficients. The interaction between dark matter and dark radiation causes the expansion rate during the matter-dominated era in the new model to be smaller than that of the Λ CDM model.

In order to facilitate model comparison, we fix the axion dark matter energy density fraction $\Omega_{\text{dm}}(z)$ at the epoch of matter-radiation equality is equal to the cold dark matter energy density fraction $\Omega_{\text{cdm}}(z)$ in the Λ CDM model. This can be achieved by adjusting the value of $\omega_{\text{dm+dr}}$ after setting the thermal friction coefficient Υ .

We compare the results obtained with thermal friction coefficients Υ of 0, 1.5, and 2.5 to those of the Λ CDM model. The four cases are represented by solid blue, dotted orange, dash-dotted green, and dashed black lines, respectively. The units of Υ are consistent with H_0 , i.e., km/s/Mpc.

In Fig. 3, the evolution of the Hubble parameter relative to the Λ CDM model as a function of the scale factor for different thermal friction coefficients are presented. In the DADM model, due to the continuous energy transfer from dark matter to dark radiation, the expansion rate during the matter-dominated era is smaller compared to the Λ CDM model. This trend persists until the dark energy domination era takes over. Moreover, the larger the thermal friction coefficient, the greater the disparity between the two models.

We demonstrate in Fig. 4 the impact on the CMB temperature power spectrum. Relative to the Λ CDM model, the thermal friction model exhibits a pronounced increase in power at low ℓ , which arises from the late-time integrated Sachs-Wolfe (ISW) effect originating from the photon passing through a time-dependent gravitational potential.

In the DADM model, due to the energy transfer from axion dark matter to dark radiation caused by thermal friction, the evolution of dark matter is modified,

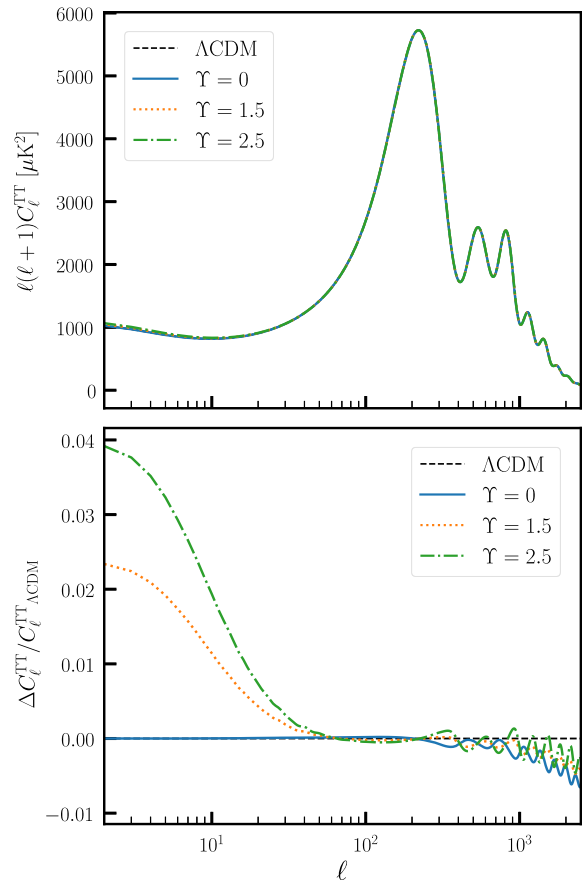


FIG. 4. The impact of various thermal friction coefficients on the CMB temperature power spectrum. The DADM model exhibits a notable impact on the CMB power spectra at low ℓ , with the spectrum significantly enhanced compared to the Λ CDM model. This variation primarily stems from the late-time ISW effect. The fluctuations at high ℓ are attributed to the diminished CMB lensing effect.

resulting in an earlier equality epoch of matter-dark energy. Consequently, this leads to a heightened late-time ISW effect.

Furthermore, the transition from dark matter to dark radiation in the DADM model leads to a reduction in CMB lensing. As a result, a decreased peak-smearing can be observed at high ℓ , resulting in a coherent trend of elevated peaks and lowered troughs compared to the Λ CDM model.

Figure 5 illustrates the results of the linear matter power spectrum relative to the Λ CDM model under different thermal friction coefficients. The dissipative nature of axion dark matter leads to a decrease in the matter density fraction Ω_m , resulting in the suppression of power. This characteristic becomes more prominent with an increase in the thermal friction coefficient. Due to fixing the energy density fraction of axion dark matter to be equal to that of cold dark matter in the Λ CDM model at the epoch of matter-radiation equality, the transition of the power spectrum is correlated with k_{eq} .

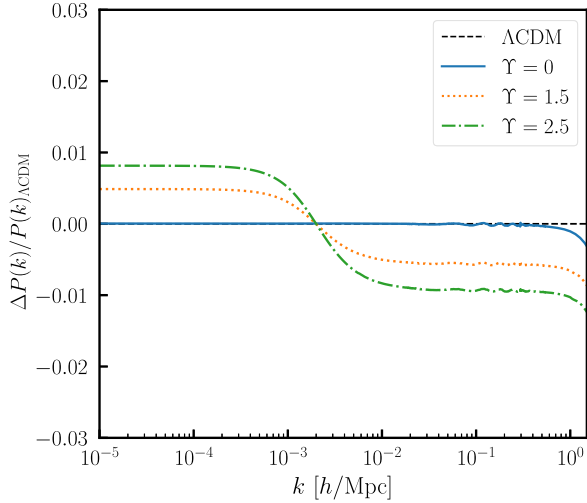


FIG. 5. The results of the linear matter power spectrum relative to the Λ CDM model are examined under different thermal friction coefficients. In the DADM model, the decrease in the matter density fraction Ω_m leads to the suppression of the $P(k)$ spectrum. Additionally, the condensation effect of axion dark matter on small scales further contributes to the suppression of the matter power spectrum.

On the smallest scale, the power spectrum of the DADM model exhibits additional reduction compared to the Λ CDM model, as evident from the curve corresponding to the blue solid line representing a thermal friction coefficient of 0. This phenomenon arises from the inherent properties of axion dark matter, specifically the condensation effect on small scales, which further suppresses the matter power spectrum.

IV. MCMC ANALYSES

We employed Cobaya [63] to perform the MCMC analysis for obtaining the posterior distribution of model parameters, and assessed the convergence using the Gelman-Rubin criterion, $R - 1 < 0.01$ [64]. The MCMC chain was analyzed using GetDist [65].

A. Datasets

We conducted our analysis using the following cosmological datasets,

- (1) *CMB*: The temperature and polarization power spectra from the *Planck* 2018 dataset, encompassing both the low- ℓ and high- ℓ observations, as well as the CMB lensing power spectrum [3,66,67].
- (2) *BAO*: The measurements from the BOSS-DR12 sample, which include the combined LOWZ and CMASS galaxy samples [68,69], as well as the small- z measurements obtained from the 6dFGS and the SDSS DR7 [70,71].
- (3) *Supernovae*: The Pantheon supernovae sample, consists of the relative luminosity distances of 1048

Type Ia supernovae, covering a redshift range from 0.01 to 2.3 [72].

By combining data from CMB and BAO, we can conduct acoustic horizon measurements at various redshifts, thereby overcoming geometric degeneracies and providing constraints on the physical processes occurring between recombination and the redshift at which BAO is measured. Moreover, the supernova data obtained from the Pantheon sample plays a crucial role in tightly constraining late-time new physic within its specific range of measured redshifts.

- (4) *SHOES*: The cosmic distance ladder measurement from SHOES with $H_0 = 73.04 \pm 1.04$ km/s/Mpc [4].
- (5) *DES*: Dark Energy Survey Year-3 weak lensing and galaxy clustering data, the application of Gaussian constraints on S_8 yields a result of 0.776 ± 0.017 [5].

We utilize the H_0 measurements from SHOES to evaluate the effectiveness of our novel model in addressing the discordance between local H_0 measurements and CMB inference results. Furthermore, we integrate the S_8 data from DES to examine the model's capability in alleviating the large-scale structure tension.

- (6) *Lyman- α* : 1D power spectrum of Lyman- α forest flux from quasar samples of SDSS DR14 BOSS and eBOSS surveys [73]. We employ a compressed version of the Gaussian prior form of the likelihood, which provides estimates for the amplitude and slope of the power spectrum at the pivot redshift of $z_p = 3$ and wave number of $k_p = 0.009$ s/km ~ 1 h/Mpc [74,75].

In addition to the commonly used datasets mentioned above, we introduced the Lyman- α data. We aim to explore the impact of small-scale measurement on the thermal friction model, as axion dark matter exhibits unique features on very small scales.

B. Results

The mean and 1σ parameter results for Λ CDM, DADM models, constrained by the combined dataset including CMB, BAO, SNIa, SHOES, and DES, are presented in Table I. Meanwhile, Table II exhibits the χ^2 statistical values.

We find that the DADM model and the Λ CDM model yield similar constraints on the value of H_0 , indicating that the ability of the thermal friction model to resolve the Hubble tension can be considered negligible.

However, the S_8 values obtained from the DADM model is smaller than that of the Λ CDM model, the value of S_8 at 68% confidence level for the DADM model is found to be 0.795 ± 0.011 , whereas the result for the Λ CDM model is 0.8023 ± 0.0085 , suggesting that the DADM model can alleviate the S_8 tension.

This effect is primarily attributed to the transfer of energy from dark matter to dark radiation in the new model,

TABLE I. The table presents the mean and 1σ marginalized constraints for Λ CDM, DADM models using a combined data comprising CMB, BAO, SNIa, SH0ES, and S_8 from DES.

| Model | Λ CDM | DADM |
|-----------------------------|------------------------------|--------------------------------|
| $\ln(10^{10}A_s)$ | $3.049^{+0.013}_{-0.015}$ | 3.054 ± 0.015 |
| n_s | 0.9705 ± 0.0036 | 0.9715 ± 0.0037 |
| τ_{reio} | $0.0595^{+0.0067}_{-0.0078}$ | $0.0608^{+0.0072}_{-0.0080}$ |
| H_0 | 68.63 ± 0.36 | 68.60 ± 0.40 |
| ω_b | 0.02259 ± 0.00013 | 0.02260 ± 0.00013 |
| $\omega_{\text{dm+dr}}$ | 0.11728 ± 0.00077 | $0.11620^{+0.0012}_{-0.00097}$ |
| $\log_{10}m_\chi$ | ... | < -21.8 |
| Υ | ... | < 2.42 |
| $10^{-9}A_s$ | $2.110^{+0.028}_{-0.032}$ | 2.119 ± 0.033 |
| Ω_m | 0.2984 ± 0.0045 | $0.2926^{+0.0066}_{-0.0056}$ |
| σ_8 | 0.8045 ± 0.0056 | 0.8048 ± 0.0059 |
| S_8 | 0.8023 ± 0.0085 | 0.795 ± 0.011 |
| $\Delta\chi^2_{\text{tot}}$ | ... | -2.60 |

resulting in a lower matter energy density fraction Ω_m . This characteristic can be more clearly observed from the posterior distributions of the model parameters for both models, as depicted in Fig. 6.

From Table II, it is observable that the performance of the DADM model and the Λ CDM model in fitting the CMB and SNIa data is comparable. While the Λ CDM model fits better with the BAO data, the DADM model matches more closely with the results from SH0ES and

TABLE II. The χ^2 statistical values for fitting a combined dataset including CMB, BAO, SNIa, SH0ES, and DES.

| Datasets | Λ CDM | DADM |
|-------------------------------|---------------|---------|
| CMB: | | |
| Planck 2018 low- ℓ TT | 22.04 | 22.67 |
| Planck 2018 low- ℓ EE | 396.10 | 397.33 |
| Planck 2018 high- ℓ | | |
| TT + TE + EE | 2352.66 | 2351.20 |
| LSS: | | |
| Planck CMB lensing | 10.17 | 9.57 |
| BAO (6dF) | 0.0017 | 0.0145 |
| BAO (DR7 MGS) | 1.86 | 2.11 |
| BAO (DR12 BOSS) | 5.858 | 6.088 |
| SNIa (Pantheon) | 1034.76 | 1034.73 |
| SH0ES | 20.55 | 18.77 |
| DES | 3.49 | 2.40 |
| $\Delta\chi^2_{\text{CMB}}$ | ... | -0.20 |
| $\Delta\chi^2_{\text{BAO}}$ | ... | 0.49 |
| $\Delta\chi^2_{\text{SNIa}}$ | ... | -0.03 |
| $\Delta\chi^2_{\text{SH0ES}}$ | ... | -1.78 |
| $\Delta\chi^2_{\text{DES}}$ | ... | -1.09 |
| $\Delta\chi^2_{\text{tot}}$ | ... | -2.60 |

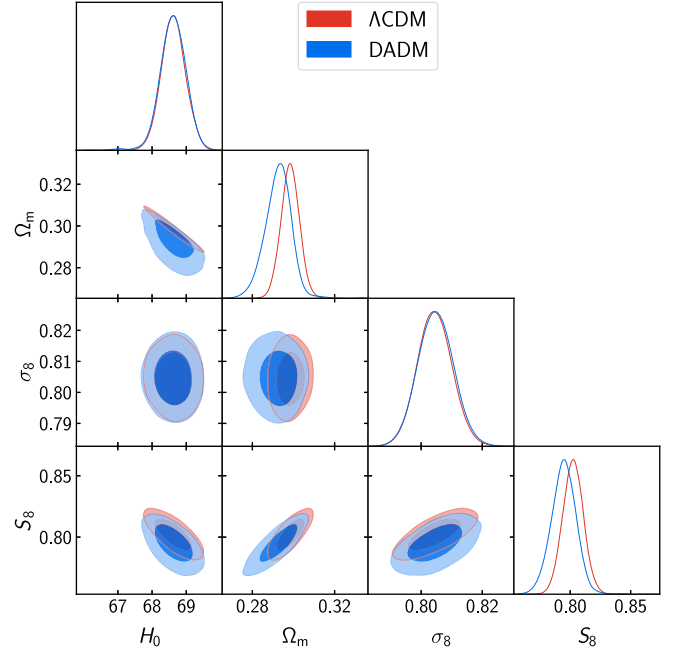


FIG. 6. The posterior distributions of selected parameters for the DADM and Λ CDM models using a combined data comprising CMB, BAO, SNIa, SH0ES, and S_8 from DES are shown. In the DADM model, dark matter undergoes energy transfer to dark radiation through thermal friction, resulting in a lower matter energy density fraction Ω_m and consequently a smaller value of S_8 .

DES. Ultimately, the DADM model yields a smaller χ^2_{tot} of -2.60 compared to the Λ CDM model.

We obtain an upper limit for the thermal friction coefficient Υ , with a maximum mean value still below 2.42 km/s/Mpc, which is consistent with our assumption of weak thermal friction. The nonzero thermal friction coefficient indicates the transfer of energy from axion dark matter to dark radiation, thereby contributing to alleviating the S_8 tension.

Moreover, we find that the mass of axion dark matter cannot be constrained when utilizing the aforementioned five datasets, as the GetDist analysis chain yielded erroneous result. Therefore, we decided to fix the mass of axion dark matter at 10^{-22} eV and investigate the impact of small-scale observation on the constraint results.

After incorporating Lyman- α data, we re-constrained the DADM model, and the constraint results from different combinations of datasets are presented in Table III. The combination of CMB, BAO, SNIa, and Lyman- α is referred to as the ‘‘Baseline’’ in our analysis.

We find that the thermal friction coefficient is still small, with its maximum result being less than 2.74 km/s/Mpc. Additionally, some slight improvements are observed, yielding values of H_0 and S_8 as $68.76^{+0.39}_{-0.35}$ km/s/Mpc and 0.791 ± 0.011 at a 68% confidence level, respectively.

TABLE III. The mean and 1σ marginalized constraints of the cosmological parameters in the DADM model based on different combinations of datasets, where we fixed the mass of axion dark matter to be 10^{-22} eV. In this context, ‘‘Baseline’’ refers to the combination of CMB, BAO, SNIa, and Lyman- α .

| Parameters | Baseline | Baseline + SH0ES | Baseline + DES | Baseline + SH0E + DES |
|-------------------------|------------------------------|------------------------------|------------------------------|------------------------------|
| $\ln(10^{10}A_s)$ | $3.057^{+0.014}_{-0.016}$ | $3.064^{+0.014}_{-0.016}$ | $3.055^{+0.013}_{-0.015}$ | $3.062^{+0.014}_{-0.016}$ |
| n_s | 0.9601 ± 0.0037 | 0.9641 ± 0.0036 | 0.9613 ± 0.0036 | 0.9646 ± 0.0038 |
| τ_{reio} | $0.0603^{+0.0069}_{-0.0079}$ | $0.0648^{+0.0072}_{-0.0083}$ | $0.0598^{+0.0067}_{-0.0077}$ | 0.0642 ± 0.0079 |
| H_0 | 67.91 ± 0.46 | $68.60^{+0.42}_{-0.37}$ | 68.22 ± 0.39 | $68.76^{+0.39}_{-0.35}$ |
| ω_b | 0.02247 ± 0.00013 | 0.02262 ± 0.00014 | 0.02251 ± 0.00014 | 0.02263 ± 0.00014 |
| $\omega_{\text{dm+dr}}$ | $0.1178^{+0.0013}_{-0.0011}$ | $0.1163^{+0.0013}_{-0.0011}$ | $0.1166^{+0.0014}_{-0.0011}$ | $0.1157^{+0.0012}_{-0.0010}$ |
| Υ | < 1.81 | < 2.06 | < 3.18 | < 2.74 |
| Ω_m | $0.3027^{+0.0073}_{-0.0066}$ | $0.2934^{+0.0073}_{-0.0063}$ | $0.2954^{+0.0077}_{-0.0062}$ | $0.2899^{+0.0066}_{-0.0059}$ |
| σ_8 | $0.8084^{+0.0057}_{-0.0065}$ | 0.8068 ± 0.0063 | 0.8047 ± 0.0055 | 0.8046 ± 0.0058 |
| S_8 | 0.812 ± 0.014 | 0.798 ± 0.013 | $0.799^{+0.011}_{-0.010}$ | 0.791 ± 0.011 |

Figure 7 shows the constraint results of the DADM model for different combinations of datasets. The complete posterior distribution, including all parameters, is illustrated in Fig. 8 in the Appendix.

The green contour represents the results obtained from the baseline dataset, which includes CMB, BAO, SNIa, and Lyman- α . The gray contour corresponds to the inclusion of the SH0ES data in addition to the baseline dataset. The red

contour represents the results obtained by adding the S_8 measurement from DES data. Lastly, the blue contour indicates the results obtained from the combination of all datasets.

It is noteworthy that when adding the SH0ES and DES data to the baseline dataset, the resulting constraints on S_8 are remarkably close, which can be explained. The effect of SH0ES data is to increase H_0 , leading to a decrease in Ω_m to maintain consistency with other data. On the other hand, DES data has the effect of reducing σ_8 without altering Ω_m . Since $S_8 \equiv \sigma_8 \sqrt{(\Omega_m/0.3)}$, despite the higher value of σ_8 from SH0ES data, the final results of S_8 obtained from both combinations of datasets are similar.

V. CONCLUSION

In this paper, we investigate the dissipative axion dark matter model as a means to alleviate cosmological tensions. In this novel model, we replace the cold dark matter with axion dark matter and introduce a coupling between the dark gauge boson and axion. This coupling leads to additional thermal friction experienced by the axion dark matter, resulting in energy injection into the dark radiation component.

The interaction between dark matter and dark radiation exhibits similarities to decaying dark matter, yet possesses distinct characteristics. We derived the evolving equations for interacting dark matter and dark radiation from a scalar field theory framework. Notably, the self-interaction of dark radiation generated by thermal friction is significantly different from the free-streaming dark radiation resulting from decaying dark matter.

We performed the MCMC analysis comparing the new model with the Λ CDM model using commonly used cosmological data, including CMB, BAO, SNIa, SH0ES, and S_8 from DES. The results indicate that the constraints on H_0 obtained from the DADM model are in close

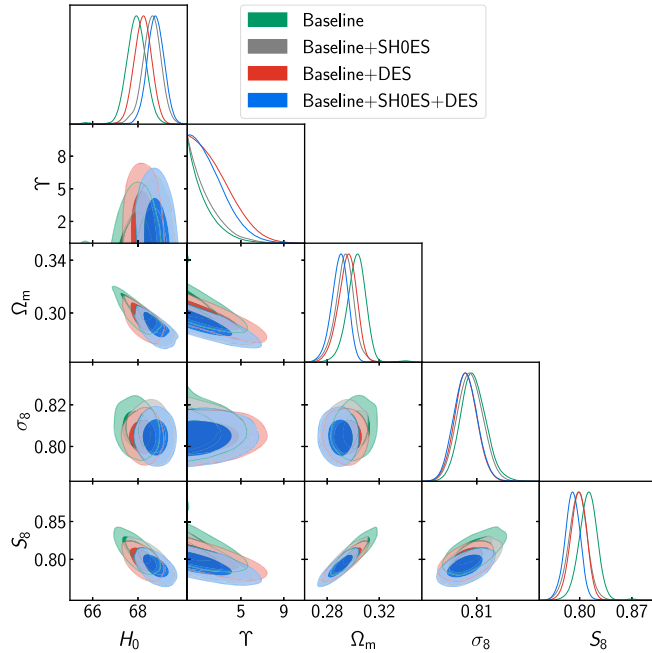


FIG. 7. Constraint results on the DADM model from different combinations of datasets are presented. The green contour represents the outcomes obtained from the baseline dataset, including CMB, BAO, SNIa, and Lyman- α . The other contours correspond to combinations of the baseline dataset with SH0ES and DES data.

agreement with those of the Λ CDM model. However, the value of S_8 in the DADM model is smaller than that in the Λ CDM model. The value of S_8 for the DADM model is found to be 0.795 ± 0.011 at a 68% confidence level, whereas the result for the Λ CDM model is 0.8023 ± 0.0085 . This suggests that the new model can partially alleviate the S_8 tension but its ability to address the Hubble tension can be ignored.

According to the χ^2 statistic, we find that the Λ CDM model provides a better fit to the BAO data, while the DADM model is more consistent with the SH0ES and DES data. Besides, there is little difference in the agreement between the two models and CMB and SNIa data. Nonetheless, the DADM model has a greater advantage in fitting the SH0ES and DES data, resulting in a smaller χ^2_{tot} of -2.60 compared to the Λ CDM model.

In addition, we found that the five aforementioned datasets are unable to constrain the mass of axion dark matter. Therefore, we fixed the mass of axion dark matter to

be 10^{-22} eV, and included small-scale data to explore its impact on the model parameters. After incorporating the Lyman- α data and performing the new round of MCMC analysis, we found that the results show slight improvements, with values of H_0 and S_8 being $68.76^{+0.39}_{-0.35}$ km/s/Mpc and 0.791 ± 0.011 at a 68% confidence level, respectively.

The axion dark matter thermal friction model still fails to fully resolve the cosmological tensions. Given that in this paper, we only consider the simplest scenario involving a constant thermal friction coefficient and the assumption of weak thermal friction, more complex models can be considered to address the Hubble and large-scale structure tensions.

ACKNOWLEDGMENTS

This work is supported in part by National Natural Science Foundation of China under Grants No. 12075042 and No. 11675032 (People's Republic of China).

APPENDIX: THE FULL MCMC POSTERiors

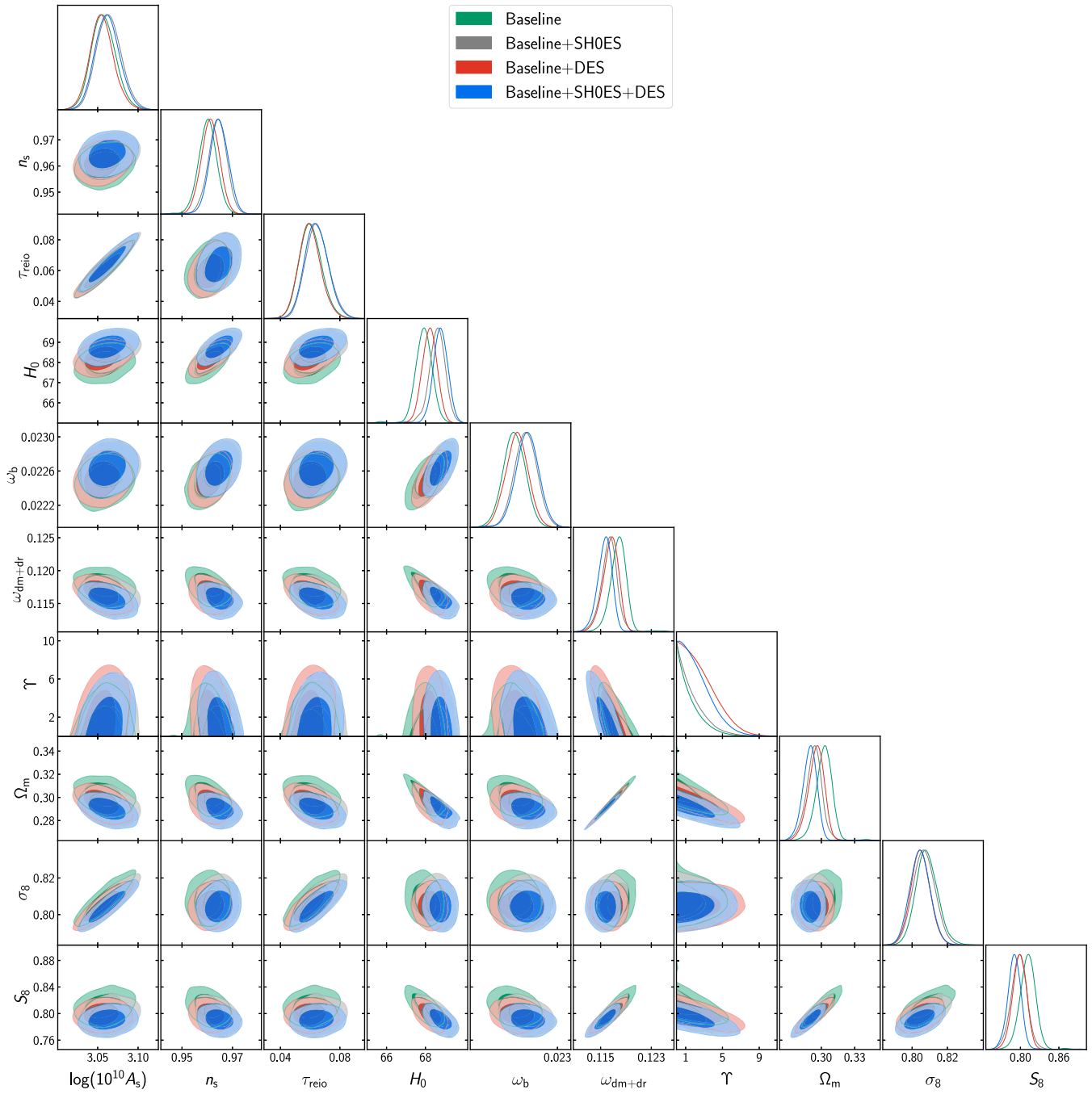


FIG. 8. The complete Markov chain Monte Carlo posterior of the DADM model parameters obtained using different combinations of datasets is presented. Various data, including CMB, BAO, SNIa, Lyman- α , SH0ES, and S_8 from DES-Y3, are utilized in our analysis.

- [1] L. Verde, T. Treu, and A. G. Riess, Tensions between the early and late universe, *Nat. Astron.* **3**, 891 (2019).
- [2] W. L. Freedman, Cosmology at crossroads: Tension with the hubble constant, *Nat. Astron.* **1**, 0121 (2017).
- [3] N. Aghanim, Y. Akrami *et al.* (Planck Collaboration), Planck 2018 results—VI. Cosmological parameters, *Astron. Astrophys.* **641**, A6 (2020).
- [4] A. G. Riess, W. Yuan, L. M. Macri *et al.*, A comprehensive measurement of the local value of the Hubble constant with 1 km/s/Mpc uncertainty from the Hubble space telescope and the SH0ES team, *Astrophys. J. Lett.* **934**, L7 (2022).
- [5] T. M. C. Abbott, M. Aguena, A. Alarcon *et al.*, Dark energy survey year 3 results: Cosmological constraints from galaxy clustering and weak lensing, *Phys. Rev. D* **105**, 023520 (2022).
- [6] X. Li and A. Shafieloo, A simple phenomenological emergent dark energy model can resolve the Hubble tension, *Astrophys. J. Lett.* **883**, L3 (2019).
- [7] Z. Zhou, G. Liu, Y. Mu, and L. Xu, Can phantom transition at $z \approx 1$ restore the Cosmic concordance?, *Mon. Not. R. Astron. Soc.* **511**, 595 (2022).
- [8] R.-Y. Guo, J.-F. Zhang, and X. Zhang, Can the H_0 tension be resolved in extensions to Λ CDM cosmology?, *J. Cosmol. Astropart. Phys.* **02** (2019) 054.
- [9] E. Di Valentino, E. V. Linder, and A. Melchiorri, Vacuum phase transition solves the H_0 tension, *Phys. Rev. D* **97**, 043528 (2018).
- [10] A. Banihashemi, N. Khosravi, and A. H. Shirazi, Ginzburg-Landau theory of dark energy: A framework to study both temporal and spatial cosmological tensions simultaneously, *Phys. Rev. D* **99**, 083509 (2019).
- [11] A. Banihashemi, N. Khosravi, and A. H. Shirazi, Phase transition in the dark sector as a proposal to lessen cosmological tensions, *Phys. Rev. D* **101**, 123521 (2020).
- [12] V. Poulin, T. L. Smith, T. Karwal, and M. Kamionkowski, Early dark energy can resolve the Hubble tension, *Phys. Rev. Lett.* **122**, 221301 (2019).
- [13] T. L. Smith, V. Poulin, and M. A. Amin, Oscillating scalar fields and the Hubble tension: A resolution with novel signatures, *Phys. Rev. D* **101**, 063523 (2020).
- [14] J. C. Hill, E. McDonough, M. W. Toomey, and S. Alexander, Early dark energy does not restore cosmological concordance, *Phys. Rev. D* **102**, 043507 (2020).
- [15] W. Yang, S. Pan, L. Xu, and D. F. Mota, Effects of anisotropic stress in interacting dark matter-dark energy scenarios, *Mon. Not. R. Astron. Soc.* **482**, 1858 (2018).
- [16] E. D. Valentino, A. Melchiorri, O. Mena, and S. Vagnozzi, Interacting dark energy in the early 2020s: A promising solution to the H_0 and cosmic shear tensions, *Phys. Dark Universe* **30**, 100666 (2020).
- [17] W. Yang, S. Pan, and A. Paliathanasis, Cosmological constraints on an exponential interaction in the dark sector, *Mon. Not. R. Astron. Soc.* **482**, 1007 (2018).
- [18] G. Liu, Z. Zhou, Y. Mu, and L. Xu, Alleviating cosmological tensions with a coupled scalar fields model, *Phys. Rev. D* **108**, 083523 (2023).
- [19] G. Liu, Z. Zhou, Y. Mu, and L. Xu, Kinetically coupled scalar fields model and cosmological tensions, [arXiv:2308.07069](https://arxiv.org/abs/2308.07069).
- [20] G. Liu, J. Gao, Y. Han, Y. Mu, and L. Xu, Mitigating cosmological tensions via momentum-coupled dark sector model, [arXiv:2310.09798](https://arxiv.org/abs/2310.09798).
- [21] M. Raveri, W. Hu, T. Hoffman, and L.-T. Wang, Partially acoustic dark matter cosmology and cosmological constraints, *Phys. Rev. D* **96**, 103501 (2017).
- [22] K. Vattis, S. M. Koushiappas, and A. Loeb, Dark matter decaying in the late universe can relieve the H_0 tension, *Phys. Rev. D* **99**, 121302 (2019).
- [23] J. Buch, P. Ralegankar, and V. Rentala, Late decaying 2-component dark matter scenario as an explanation of the AMS-02 positron excess, *J. Cosmol. Astropart. Phys.* **10** (2017) 028.
- [24] T. Bringmann, F. Kahlhoefer, K. Schmidt-Hoberg, and P. Walia, Converting nonrelativistic dark matter to radiation, *Phys. Rev. D* **98**, 023543 (2018).
- [25] S. J. Clark, K. Vattis, and S. M. Koushiappas, Cosmological constraints on late-universe decaying dark matter as a solution to the H_0 tension, *Phys. Rev. D* **103**, 043014 (2021).
- [26] K. L. Pandey, T. Karwal, and S. Das, Alleviating the H_0 and σ_8 anomalies with a decaying dark matter model, *J. Cosmol. Astropart. Phys.* **07** (2020) 026.
- [27] S. Alvi, T. Brinckmann, M. Gerbino, M. Lattanzi, and L. Pagano, Do you smell something decaying? Updated linear constraints on decaying dark matter scenarios, *J. Cosmol. Astropart. Phys.* **11** (2022) 015.
- [28] F. McCarthy and J. C. Hill, Converting dark matter to dark radiation does not solve cosmological tensions, *Phys. Rev. D* **108**, 063501 (2023).
- [29] Z. Zhou, G. Liu, Y. Mu, and L. Xu, Limit on the dark matter mass from its interaction with photons, *Phys. Rev. D* **105**, 103509 (2022).
- [30] F. D’Eramo, R. Z. Ferreira, A. Notari, and J. L. Bernal, Hot axions and the H_0 tension, *J. Cosmol. Astropart. Phys.* **11** (2018) 014.
- [31] A. El-Zant, W. E. Hanafy, and S. Elgammal, H_0 tension and the phantom regime: A case study in terms of an infrared $f(t)$ gravity, *Astrophys. J.* **871**, 210 (2019).
- [32] N. Khosravi, S. Baghran, N. Afshordi, and N. Altamirano, H_0 tension as a hint for a transition in gravitational theory, *Phys. Rev. D* **99**, 103526 (2019).
- [33] J. Renk, M. Zumalacárregui, F. Montanari, and A. Barreira, Galileon gravity in light of ISW, CMB, BAO and H_0 data, *J. Cosmol. Astropart. Phys.* **10** (2017) 020.
- [34] M. Braglia, M. Ballardini, W. T. Emond, F. Finelli, A. E. Gümrükçüoğlu, K. Koyama, and D. Paoletti, Larger value for H_0 by an evolving gravitational constant, *Phys. Rev. D* **102**, 023529 (2020).
- [35] L. O. Téllez-Tovar, T. Matos, and J. A. Vázquez, Cosmological constraints on the multiscalar field dark matter model, *Phys. Rev. D* **106**, 123501 (2022).
- [36] E. G. M. Ferreira, Ultra-light dark matter, *Astron. Astrophys. Rev.* **29**, 7 (2021).
- [37] L. A. Ureña-López and A. X. Gonzalez-Morales, Towards accurate cosmological predictions for rapidly oscillating scalar fields as dark matter, *J. Cosmol. Astropart. Phys.* **07** (2016) 048.
- [38] F. X. L. Cedeño, A. X. González-Morales, and L. A. Ureña-López, Cosmological signatures of ultralight dark matter

- with an axionlike potential, *Phys. Rev. D* **96**, 061301 (2017).
- [39] A. Berera, Warm inflation, *Phys. Rev. Lett.* **75**, 3218 (1995).
- [40] A. Berera and L.-Z. Fang, Thermally induced density perturbations in the inflation era, *Phys. Rev. Lett.* **74**, 1912 (1995).
- [41] A. Berera, I. G. Moss, and R. O. Ramos, Warm inflation and its microphysical basis, *Rep. Prog. Phys.* **72**, 026901 (2009).
- [42] M. Bastero-Gil, A. Berera, R. O. Ramos, and J. a. G. Rosa, Warm little inflaton, *Phys. Rev. Lett.* **117**, 151301 (2016).
- [43] K. V. Berghaus, P. W. Graham, and D. E. Kaplan, Minimal warm inflation, *J. Cosmol. Astropart. Phys.* **03** (2020) 034.
- [44] P. W. Graham, D. E. Kaplan, and S. Rajendran, Relaxation of the cosmological constant, *Phys. Rev. D* **100**, 015048 (2019).
- [45] K. V. Berghaus, P. W. Graham, D. E. Kaplan, G. D. Moore, and S. Rajendran, Dark energy radiation, *Phys. Rev. D* **104**, 083520 (2021).
- [46] K. V. Berghaus and T. Karwal, Thermal friction as a solution to the hubble tension, *Phys. Rev. D* **101**, 083537 (2020).
- [47] K. V. Berghaus and T. Karwal, Thermal friction as a solution to the hubble and large-scale structure tensions, *Phys. Rev. D* **107**, 103515 (2023).
- [48] J. Beyer and C. Wetterich, Small scale structures in coupled scalar field dark matter, *Phys. Lett. B* **738**, 418 (2014).
- [49] L. Amendola and R. Barbieri, Dark matter from an ultra-light pseudo-goldstone-boson, *Phys. Lett. B* **642**, 192 (2006).
- [50] M. Bastero-Gil, A. Berera, I. G. Moss, and R. O. Ramos, Theory of non-Gaussianity in warm inflation, *J. Cosmol. Astropart. Phys.* **12** (2014) 008.
- [51] L. McLerran, E. Mottola, and M. E. Shaposhnikov, Sphalerons and axion dynamics in high-temperature QCD, *Phys. Rev. D* **43**, 2027 (1991).
- [52] G. D. Moore and M. Tassler, The sphaleron rate in SU(n) gauge theory, *J. High Energy Phys.* **02** (2011) 105.
- [53] M. Laine and A. Vuorinen, *Basics of Thermal Field Theory* (Springer International Publishing, New York, 2016), 10.1007/978-3-319-31933-9.
- [54] E. J. Copeland, A. R. Liddle, and D. Wands, Exponential potentials and cosmological scaling solutions, *Phys. Rev. D* **57**, 4686 (1998).
- [55] B. Audren, J. Lesgourgues, G. Mangano, P. D. Serpico, and T. Tram, Strongest model-independent bound on the lifetime of dark matter, *J. Cosmol. Astropart. Phys.* **12** (2014) 028.
- [56] J. Lesgourgues, G. Marques-Tavares, and M. Schmaltz, Evidence for dark matter interactions in cosmological precision data?, *J. Cosmol. Astropart. Phys.* **02** (2016) 037.
- [57] P. G. Ferreira and M. Joyce, Cosmology with a primordial scaling field, *Phys. Rev. D* **58**, 023503 (1998).
- [58] W. Hu, Structure formation with generalized dark matter, *Astrophys. J.* **506**, 485 (1998).
- [59] V. Poulin, P. D. Serpico, and J. Lesgourgues, A fresh look at linear cosmological constraints on a decaying dark matter component, *J. Cosmol. Astropart. Phys.* **08** (2016) 036.
- [60] T. Simon, G. F. Abellán, P. Du, V. Poulin, and Y. Tsai, Constraining decaying dark matter with boss data and the effective field theory of large-scale structures, *Phys. Rev. D* **106**, 023516 (2022).
- [61] J. Lesgourgues, The cosmic linear anisotropy solving system (class) I: Overview, [arXiv:1104.2932](https://arxiv.org/abs/1104.2932).
- [62] D. Blas, J. Lesgourgues, and T. Tram, The cosmic linear anisotropy solving system (CLASS). Part II: Approximation schemes, *J. Cosmol. Astropart. Phys.* **07** (2011) 034.
- [63] J. Torrado and A. Lewis, Cobaya: Code for Bayesian analysis of hierarchical physical models, *J. Cosmol. Astropart. Phys.* **05** (2021) 057.
- [64] A. Gelman and D. B. Rubin, Inference from iterative simulation using multiple sequences, *Stat. Sci.* **7**, 457 (1992).
- [65] A. Lewis, GetDist: A PYTHON package for analysing Monte Carlo samples, [arXiv:1910.13970](https://arxiv.org/abs/1910.13970).
- [66] N. Aghanim, Y. Akrami, M. Ashdown *et al.*, Planck 2018 results. V. CMB power spectra and likelihoods, *Astron. Astrophys.* **641**, A5 (2020).
- [67] N. Aghanim, Y. Akrami, M. Ashdown *et al.*, Planck 2018 results—VIII. Gravitational lensing, *Astron. Astrophys.* **641**, A8 (2020).
- [68] S. Alam, M. Ata, S. Bailey *et al.*, The clustering of galaxies in the completed SDSS-III baryon oscillation spectroscopic survey: Cosmological analysis of the DR12 galaxy sample, *Mon. Not. R. Astron. Soc.* **470**, 2617 (2017).
- [69] M. A. Buen-Abad, M. Schmaltz, J. Lesgourgues, and T. Brinckmann, Interacting dark sector and precision cosmology, *J. Cosmol. Astropart. Phys.* **01** (2018) 008.
- [70] F. Beutler, C. Blake, M. Colless, D. Heath Jones, L. Staveley-Smith, L. Campbell, Q. Parker, W. Saunders, and F. Watson, The 6dF Galaxy Survey: Baryon acoustic oscillations and the local Hubble constant, *Mon. Not. R. Astron. Soc.* **416**, 3017 (2011).
- [71] A. J. Ross, L. Samushia, C. Howlett, W. J. Percival, A. Burden, and M. Manera, The clustering of the SDSS DR7 main galaxy sample—i. a 4 percent distance measure at $z = 0.15$, *Mon. Not. R. Astron. Soc.* **449**, 835 (2015).
- [72] D. M. Scolnic, D. O. Jones, A. Rest, Y. C. Pan *et al.*, The complete light-curve sample of spectroscopically confirmed SNe ia from pan-STARRS1 and cosmological constraints from the combined pantheon sample, *Astrophys. J.* **859**, 101 (2018).
- [73] S. Chabanier, N. Palanque-Delabrouille, C. Yèche *et al.*, The one-dimensional power spectrum from the sdss dr14 1α forests, *J. Cosmol. Astropart. Phys.* **07** (2019) 017.
- [74] S. Goldstein, J. C. Hill, V. Iršič, and B. D. Sherwin, Canonical hubble-tension-resolving early dark energy cosmologies are inconsistent with the lyman- α forest, *Phys. Rev. Lett.* **131**, 201001 (2023).
- [75] A. He, R. An, M. M. Ivanov, and V. Gluscevic, Self-interacting neutrinos in light of large-scale structure data, [arXiv:2309.03956](https://arxiv.org/abs/2309.03956).